Progress in Natural Science: Materials International 2012;22(2):108–114

Chinese Materials Research Society

Progress in Natural Science: Materials International

www.elsevier.com/locate/pnsmi
www.sciencedirect.com

ORIGINAL RESEARCH

# Preparation of composite tubular grafts for vascular repair via electrospinning

**Chen Huang[a,b], Xiaohua Geng[a], Qinfei Ke[b], Xiumei Mo[a,*], Salem S. Al-Deyab[c], Mohamed El-Newehy[c,d]**

[a]*Biomaterials and Tissue Engineering Laboratory, College of Chemistry, Chemical Engineering and Biotechnology, Donghua University, Shanghai 201620, China*
[b]*College of Textiles, Donghua University, Shanghai 201620, China*
[c]*Petrochemical Research Chair, Department of Chemistry, College of Science, King Saud University, Riyadh 11451, Saudi Arabia*
[d]*Department of Chemistry, Faculty of Science, Tanta University, Tanta 31527, Egypt*

Received 19 November 2011; accepted 18 January 2012
Available online 3 April 2012

**KEYWORDS**

Electrospinning;
Composite;
Vascular graft;
Endothelial cell;
Nanofiber

**Abstract** A novel type of composite vascular graft was developed via electrospinning in the present investigation. Collagen and chitosan were blended to form the inner and outer layer. Poly(l-lactide-co-caprolactone) (P(LLA-CL)) was selected as a material for the middle layer of composite vascular graft. Both morphology and diameter of the composite grafts were studied by Scanning Electron Microscope (SEM). The results of mechanical tests showed that the composite scaffolds provided the whole grafts with better strength and flexibility compared with blended grafts, mainly due to the fact that the middle layer was P(LLA-CL). Cell viability studies with endothelial cells suggested a prompt adhesion and proliferation duo to the fact that the outer layer was collagen and chitosan. Confocal microscopy demonstrated that a monolayer of endothelial cells could be formed after 7 days of culture. The above results indicated that the composite fibrous scaffolds could be a good candidate for blood vessel repair by electrospinning method.

© 2012. Chinese Materials Research Society. Production and hosting by Elsevier Ltd. All rights reserved.

*Corresponding author. Tel.: +86 21 67792653.
E-mail address: xmm@dhu.edu.cn (X.M. Mo).

1002-0071 © 2012. Chinese Materials Research Society. Production and hosting by Elsevier Ltd. All rights reserved.

Peer review under responsibility of Chinese Materials Research Society.
doi:10.1016/j.pnsc.2012.03.005

Production and hosting by Elsevier

## 1. Introduction

Cardiovascular disease remains the major cause of mortality worldwide today. In the United States alone, around 81 million adults (more than 1 in 3) have 1 or more types of cardiovascular diseases, among them 38 million are estimated to be older than 60 [1]. In those cases, the use of prosthetic vascular grafts is of extreme importance as suitable autologous substitutions may not be available due to aging or other problems. To find qualified vascular replacement without hurting other parts of the patient's body, there comes the subject of vascular tissue engineering.

As a burgeoning technology, tissue engineering is a interdisciplinary subject that combines genetic engineering of cells with chemical engineering to create artificial organs and tissues, such as skin, bones, blood vessels and nerve conduits [2]. The main challenge for tissue engineering scaffolds is to design and fabricate customizable biodegradable matrices that can mimic the componential and structural aspects of native extracellular matrices (ECM) [3].

Collagen and chitosan were selected in this study to biomimetic the natural ECM from the component point of view and electrospinning technique was employed with the hope to match the structure of nanofibrous membranes in ECM. As the main protein of connective tissue in animals and the most abundant protein in mammals, collagen is widely used as starting materials in biomedical fields. Chitosan, a massive natural polysaccharide derived from chitin, has an analogous structure with glycosaminoglycan, which is the main component of natural ECM [4,5]. Both of the above have good biocompatibility, appropriate biodegradability and commercial availability.

Moreover, despite successful applications of synthetic polymers (Dacron, PTFE, etc.) in the replacement of large diameter ($>6$ mm) vascular grafts [6], for small-diameter ($<6$ mm) vascular bypass grafts, those materials are of limited usage due to acute thrombogenicity, aneurysm formation and other problems related to immune response [7]. Therefore, efforts have been made to develop natural materials-based scaffolds using collagen [8–10], chitosan [11,12], gelatin [13,14], silk fibroin [15,16] and other biocompatible natural materials [17,18]. Unfortunately, although in-depth researches have been conducted through these kinds of materials, there remains a non-ignorable gap between lab activities and clinical trials for the application of natural materials, as most of them are too fragile to provide sufficient mechanical strength. Thus, at present stage researchers are inclined to blend natural materials with synthetic polymers in the design and fabrication of vascular grafts.

Compared to pure natural materials, natural–synthetic blends have the possibility to provide enough mechanical strength. Meanwhile, with certain balance, the negative influence of synthetic materials on cell proliferation and differentiation could be reduced to a large extent [19]. Practicable as this approach might be, to date there is no clear consensus as to what method, material and blend ratio – past, present or future – could lead to a clinically applicable treatment. As some kind of compromise between pure natural or synthetic materials, their blends do not have the potential to thoroughly avoid problems like mechanical deficiency and poor biocompatibility at the blood–material interface. Moreover, such a simple blending structure could not match the multiple stresses including circumferential, longitudinal, torsional and shear of native arteries.

In this study, a simple electrospinning method was adopted to prepare a three-layered nanofibrous tube. The inner and outer layers of the tubular grafts were formed by collagen and chitosan. Poly (l-lactide-co-ε-caprolactone) P(LLA-CL), a copolymer of PLLA and PCL [75:25], served as a material for the middle layer. Mechanical properties showed that the composite scaffolds possessed better strength and flexibility compared with the blended scaffolds. Cell proliferation rate on collagen–chitosan fibers was higher without synthetic polymers contacted by the cells. The above results suggest that the composite vascular scaffolds made of collagen, chitosan and P(LLA-CL) might be a candidate for vascular repair.

## 2. Experimental

### 2.1. Starting materials

Water soluble collagen I (mol. wt., $0.8–1 \times 10^5$ Da) was purchased from Sichuan Ming-rang Bio-Tech Co., Ltd. (China), chitosan (85%, deacetylated, $M_\eta \approx 10^6$) was purchased from Ji-nan Haidebei Marine Bioengineering Co., Ltd. (China) and a copolymer of P(LLA-CL) (75:50), which has a composition of 50 mol% L-lactide, was used. Two types of solvents, 1,1,1,3,3,3-hexafluoroisopropanol (HFIP) from Fluorochem Ltd. (UK) and trifluoroacetic acid (TFA) from Sinopharm Chemical Reagent Co., Ltd. (China) were used to dissolve the collagen, chitosan, P(LLA-CL) and their blends, respectively. A crosslinking agent of aqueous glutaraldehyde (GTA) solution (25%) was purchased from Sinopharm Chemical Reagent Co., Ltd. (China). Rat endothelial cells were donated from Barwon Hospital, Australia. All reagents were purchased from Gibco Life Technologies, USA unless specified.

### 2.2. Preparation of the scaffolds

Collagen (8 wt%) and P(LLA-CL) (10 wt%) were dissolved in HFP while chitosan (8 wt%) was dissolved in HFP/TFA mixture (v/v, 90/10). To fabricate the inner and outer layers of composite grafts, collagen and chitosan were blended with a weight ratio of 4/1. Both layers were electrospun by 1.5 ml of mixed solution while 1 ml of P(LLA-CL) solution was electrospun as the mid-layer. All the solutions were filled into 2.5 ml plastic syringes with a blunt-ended needle. The syringe was attached to a syringe pump (789100C, Cole-Pamer, USA) and dispensed at a rate of 1.0 ml/h. A voltage of 18 kV was obtained from a high voltage power supply (BGG6-358, BMEICO. Ltd., China) and applied across the needle and ground collector (a 3 mm diameter mandrel with a rotating speed of 300 rpm). In accordance with the diameter of the mandrel, the inner diameter of the tubular grafts was 3 mm. For comparison, membranes and blended tubular grafts made by collagen/chitosan/P(LLA-CL) blends were electrospun with a blending weight ratio of 60%/15%/25% (in consistency with the proportion used in fabricating composite grafts). After electrospinning, samples were crosslinked in a sealed desiccator containing 10 ml of 25% glutaraldehyde (GTA) aqueous solution for various periods of time.

### 2.3. Characterization

The morphology of the final products was characterized SEM using a JSM-5600 scanning electronic microscope (Japan). The tubular scaffolds were immersed into liquid nitrogen and

rapidly cut using a scalpel to generate a cross-section in which the edge of the layers could be seen. Fiber diameter and layer thickness were estimated using image analysis software (Image-J, National Institutes of Health, U.S.A). Pore size was measured by cutting the membrane samples ($n=6$) into $3 \times 3\ cm^2$ and a CFP-1100-AI capillary flow porometer (PMI Porous Materials Int.) was used to measure pore size and pore distribution. Mechanical testing was performed using a universal materials tester (H5 K-S, Hounsfield, UK) with a 50 N load cell at ambient temperature 20 °C and humidity 65%. A cross-head speed of 10 mm/min was used for all the specimens tested. All specimens were tested to failure.

For multi-layered and blended tubular grafts, tensile tests were performed by cutting the grafts along their longitudinal directions into a uniform size ($30 \times 5\ mm^2$). The specimen thicknesses were measured using a micrometer having a precision of 0.01 mm. The machine-recorded data were used to process the tensile stress–strain curves of the specimens.

### 2.4. Cell morphology and viability

Rat endothelial cells were cultured in DMEM medium with 10% fetal bovine serum and 1% antibiotic–antimycotic in an atmosphere of 5% $CO_2$ and 37 °C, and the medium was replenished every three days. Before seeding cells, scaffolds were sterilized by immersing in 75% ethanol for 2 h, washed 3 times with phosphate-buffered saline solution (PBS), and then washed once with the culture medium.

Cell viability was assayed with cell counting kit-8 (CCK-8, Sigma-Aldrich). Briefly, all the scaffolds were rinsed, moved to another 24-well tissue culture polystyrene (TCP), and immersed with 400 ml of fresh culture medium in each well. Forty microliters of CCK-8 reagent was added into each well and incubated for 2 h according to the reagent instruction, and the same volumes of culture medium and CCK-8 reagent without cells were also incubated as the background. An aliquot (150 ml) of incubated medium was pipetted into a 96-well TCP, and the absorbance at 450 nm was measured for each well as above. The cell proliferation was examined on days 1, 3 and 7 after incubation. TCP wells were seeded as control and all experiments were performed with $n=6$.

For observing cells under confocal microscope, the cultured matrices were first washed with sterilized PBS for three times to remove medium and unviable cells, followed by immersing in PBS solution containing 2% paraformaldehyde for 10 min at room temperature. After rinsing with PBS for three times, the matrices were placed in a permeabilization solution (0.2% Triton X-100, Sigma-Aldrich) at room temperature for 10 min and rinsed again with fresh PBS for three times. The matrices were then stained with 4,6-diamidino-2-phenylindole and phalloidin alexa 568 overnight before observation.

### 2.5. Statistics analysis

Statistics analysis was performed using origin 7.5 (Origin lab Inc., USA). Values (at least triplicate) were averaged and expressed as means ± standard deviation (SD). Statistical differences were determined by the analysis of One-Way ANOVA and differences were considered statistically significant at $p<0.05$.

## 3. Results and discussion

### 3.1. Morphology and pore size

Three-step single electrospinning was employed to fabricate composite grafts. The inner and outer layers of the graft were formed by 1.5 ml 8% collagen/chitosan while the mid-layer was formed by 1 ml 8% P(LLA-CL) (Fig. 1A). Cross-sectional SEM image in Fig. 1B shows the edge of each layer, demonstrating the existence of 3 different layers. Although the whole scaffold had been immersed into liquid nitrogen before cutting, P(LLA-CL) fibers could not be easily cut off by the scalpel due to their high elasticity. A stretching behavior might have occurred during the cutting process, resulted in a morphological difference between P(LLA-CL) and collagen/chitosan cross-sectional images, as stressed by the inset pictures in Fig. 1B.

For the comparison of fiber morphology, collagen/chitosan blended solution was directly electrospun on a plain aluminum foil, after which a very thin layer of P(LLA-CL) fibers was electospun and deposited on the mat to form a bi-layered membrane. Surface morphologies of the fibrous membrane were shown in Fig. 2A and B, and morphologies of collagen/chitosan/P(LLA-CL) blends (blending weight ratio =60%/15%/25%, same as their composite counterparts) can be observed from Fig. 2C and D.

Fig. 2A and B apparently shows the difference between the inner (outer) layer and mid-layer of the composite vascular scaffold. Diameter of the upper P(LLA-CL) fibers and the

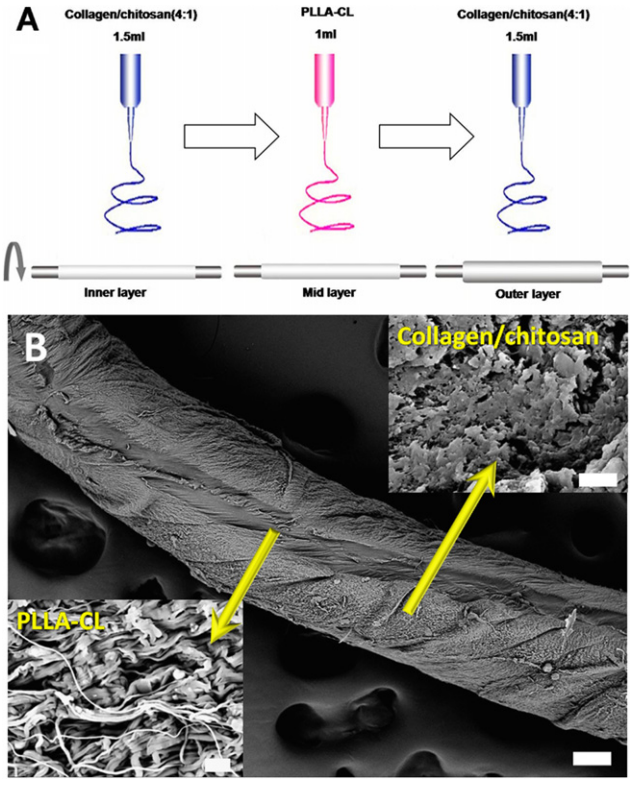


**Fig. 1** (A) Schematic diagram of the 3-step electrospinning processes. (B) SEM images of 3-layerd composite graft and its cross section (inset). Scale bar (main picture) = 100 μm, scale bar (inset) = 2 μm.

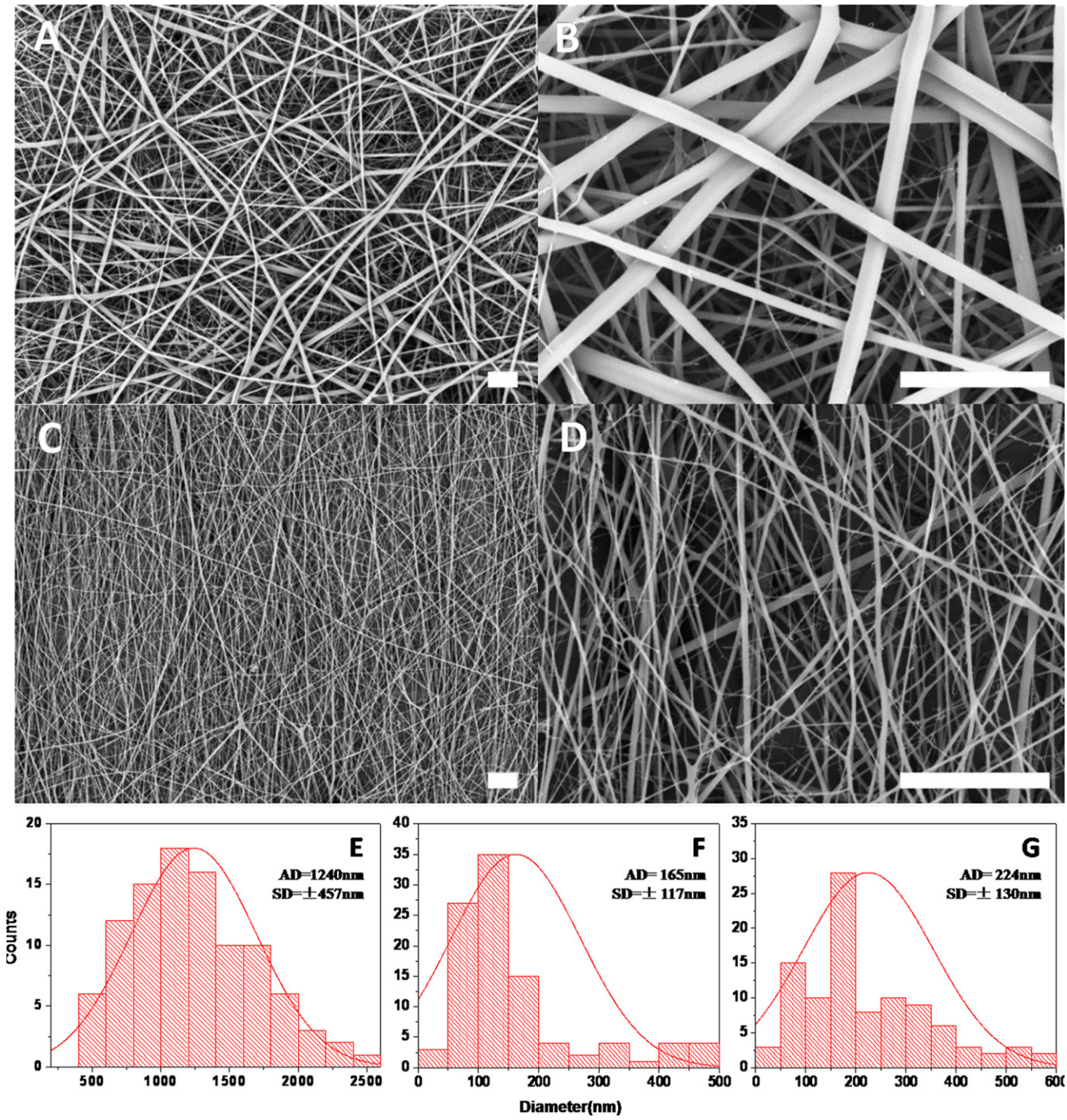


**Fig. 2** SEM images of collagen/chitosan/P(LLA-CL) nanofibers under different magnifications and their diameter distribution: (A), (B) collagen/chitosan fibers at the bottom and P(LLA-CL) fibers on the top; (C), (D) blended collagen/chitosan/P(LLA-CL) fibers. (E), (F) and (G) Diameter distribution of pure P(LLA-CL), collagen/chitasan, and collagen/chitosan/P(LLA-CL) blended fibers, respectively. Scale bar = 10 μm.

bottom collagen/chitosan fibers were observed in the range of $1240 \pm 457$ and $165 \pm 117$ nm, respectively (Fig. 2E and F). Although most P(LLA-CL) fibers have a diameter range from 0.8 to 2.0 μm, when mixed with collagen and chitosan, the acquired fibers were much thinner with an estimated diameter of $224 \pm 130$ nm (Fig. 2G).

Comparing the curves in Fig. 2E and F, it is clearly seen that the diameter of electrospun P(LLA-CL) fibers was more evenly distributed than that of collagen/chitosan ones. This is probably due to the positive charges carried by chitosan. Since the stretching of solution could be ascribed to the repulsive forces between the charges on electrospinning jet, these positive charges would enhance the stretching behavior by increasing solution conductivity. This could also be an explanation of why P(LLA-CL) fibers became much thinner when it was electrospun together with collagen and chitosan.

Apart from positive charges, concentration of P(LLA-CL) decreased from 8 to 2 wt% in the blended solution, making the polymer easier to be stretched by electrical force, thus, no micrometer-scaled P(LLA-CL) fibers (Fig. 2B) could be found from Fig. 2D.

As a widely used method to stabilize scaffolds, GTA vapor crosslinking can prevent collagen and chitosan from being dissolved in water while holding no significant impacts on fiber diameter except forming some bonds at fiber junctions [4,20]. One of the key factors in this process is the crosslinking time. Depending on material properties and scaffold thickness, different crosslinking time should be employed to find a balance between stability and morphology. For one thing, when the duration was too long (72 h in this study), fibers intended to stick with each other and fiber morphology could be damaged, as shown in Fig. 3C; for another, without sufficient crosslinking fibers (24 h in this study) could be easily dissolved in aqueous solution, as shown in Fig. 3D. When immersed in 37 °C PBS for 4 days, most of the 24 h-crosslinked fibers were swelled that no pores remained on the surface of the scaffold. After a few trials, a suitable crosslinking time of 60 h was set in regard to the sample thickness (0.3–0.4 mm).

When crosslinking was over, the scaffolds became yellowish and shrank slightly dimensionally which can cause changes of pore size and wall thickness. It is clear as shown in Fig. 3A and B, that the length of tubular graft decreased from 1.6 to 0.9 cm without obvious fixation. However, if the two edges were fixed, decrease in wall thickness occurred to offset the shrinkage in length. Table 1 shows the thickness and pore size change of both blended and composite grafts before and after crosslinking. Due to the existence of P(LLA-CL) microfibers, pore size of composite scaffolds was comparatively larger than that of blended scaffolds, which could be conducive to cells for the reason that apart from fiber diameter, pore size of tissue-engineered scaffolds also plays an important role. Those microscale and nanoscale porous structure helps to facilitate the passage of nutrients and the exchange of gases, which are crucial for cellular growth and tissue regeneration [21]. However, when the crosslinking process was over, a decrease in thickness and pore size of the blended scaffold was observed. This was probably caused by the bonds formed at fiber junctions during the stabilization.

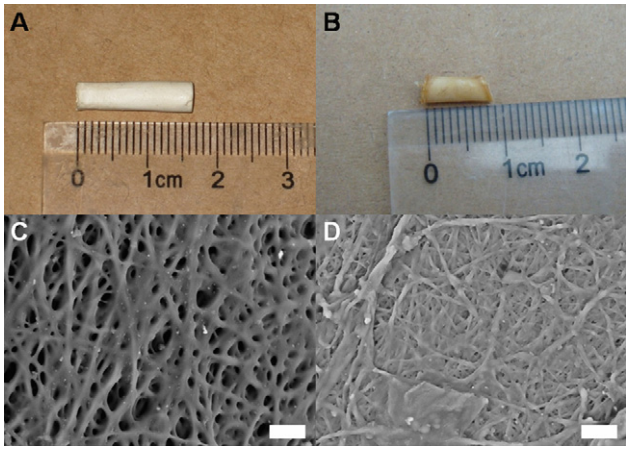


**Fig. 3** Macrographic images of electrospun tubular graft before (A) and after (B) crosslinking; (C) SEM micrographs of 72 h-crosslinked collagen/chitosan fibers, (D) 24 h crosslinked collagen/chitosan fibers after being immersed in PBS solution at 37 °C for 4 days. Scale bar = 10 μm.

### 3.2. *Mechanical properties*

The tensile stress–strain curves of electrospun pure P(LLA-CL), blended and composite collagen/chitosan/P(LLA-CL) fibers are shown in Fig. 4. As expected, scaffolds made of pure P(LLA-CL) had the superior performance in both strength (~8 Mpa in stress) and flexibility (~220% in strain), while blended ones had the stress lower than 5 Mpa and the strain less than 70%. This is reasonable as the mechanical properties of fibrous mat depend largely on the mechanical properties of the single fibers and the interactions among the fibers making up the mat. Composite scaffolds experienced two different stages during the tensile processes. At first, the initial modulus was highly matched with that of blended scaffolds, which can be attributed to the same composition ratio of collagen, chitosan and P(LLA-CL). When this stage was over, typical mechanical properties of P(LLA-CL) was shown on the curve, which might be explained by the fact that during the measurement, a lot of tiny cracks were observed from the surface of the sample. Such phenomenon suggests the breakage of collagen/chitosan fibers, as they formed both the inner and outer surfaces.

While it is evident that the biocompatibility plays a major role in achieving patent vessels, vascular scaffolds which serve as cell carriers and provide structural support contribute to the ultimate success of engineered grafts [22]. Due to the high elasticity of P(LLA-CL), the composite graft in our study had a better mechanical performance than their blended counterparts. It also had a much larger strain when compared to other natural–synthetic blended vascular scaffolds [23–25], indicating a higher flexibility that is particularly desired in blood vessel tissue engineering. Moreover, the mechanical properties could be further tailored to meet the requirement of other specific applications via changing the blending weight ratio of P(LLA-CL) and collagen/chitosan.

**Table 1** Pore diameters of blended and composite collagen/chitosan/P(LLA-CL) fibrous scaffolds.

| Scaffolds ($n=6$) | | Specimen thickness (mm) | Mean flow pore diameter ± SD (μm) | Largest pore diameter (μm) | Smallest pore diameter (μm) |
|---|---|---|---|---|---|
| Blended | Non-crosslinked | 0.360 | 0.1463 ± 0.0292 | 0.4199 | 0.0723 |
| | Crosslinked | 0.304 | 0.1002 ± 0.0215 | 0.2568 | 0.0438 |
| Composite | Non-crosslinked | 0.389 | 0.2077 ± 0.0780 | 0.6936 | 0.1578 |
| | Crosslinked | 0.357 | 0.1534 ± 0.0441 | 0.5059 | 0.0681 |

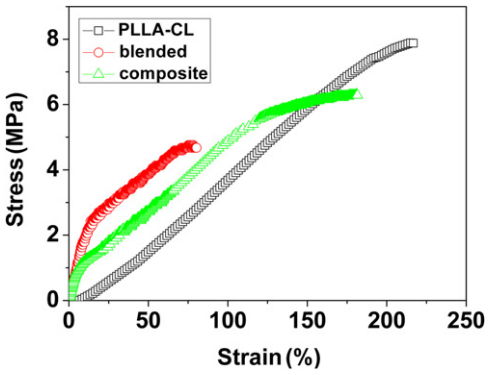


**Fig. 4** Stress–strain curves of the scaffolds made of pure P(LLA-CL), blended and composite collagen/chitosan/P(LLA-CL) fibers, respectively.

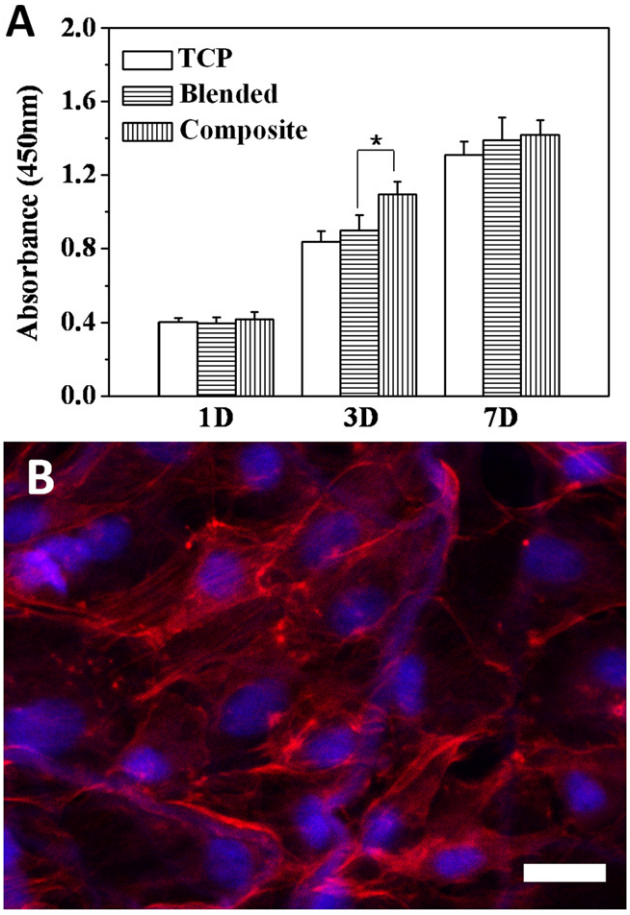


**Fig. 5** (A) Cell viability after seeding measured for 1, 3 and 7 day, (B) Confocal image of endothelial cells on the composite scaffolds for day 7. Scale bar = 25 μm.

### 3.3. *Morphology and viability of cell*

Scaffolding materials for tissue engineering approaches are typically designed to promote cell growth, physiological functions and maintain normal states of cell differentiation [26–28]. Rat endothelial cells were seeded to evaluate cell proliferation on the electrospun nanofibrous scaffolds. Cell viability after seeding for days 1, 3, and 7 on different scaffolds is shown in Fig. 5A. Both blended and composite scaffolds showed a prompt proliferation, which was possibly caused by the introduction of biological functional groups via collagen and chitosan. At the culture time of day 1, no significant difference could be found among the scaffolds. Whereas for day 3, a dramatical increase ($P \leq 0.05$) of cell proliferation value on the composite scaffolds was observed in comparison with the other two scaffolds. Such a phenomenon suggests that hydrophilic surface made of pure natural materials might be more desirable for cell growth. For day 7, although total cell number still increased, the proliferation rate on the composite scaffolds was lower than those of blended scaffolds and TCP. This is probably due to the insufficiency of space, which could be demonstrated by the confocal image shown in Fig. 5B. No enough space could support further growth due to the entire surface covered by a cell monolayer although it had a better biocompatibility for the well-spread endothelial cells. To sum up, a faster growth speed of endothelial cells was measured on the surface of natural materials when no synthetic material was blended.

## 4. Conclusions

In this study, a composite vascular graft was electrospun by using collagen and chitosan as the inner and outer layer, and P(LLA-CL) as the middle layer. Fiber diameters varied dramatically in respond to different polymer solutions. Both mechanical properties and biocompatibility of the composite scaffolds were better than those of blended counterparts, therefore, the composite fibrous scaffolds could be a better candidate for blood vessel repair.

## Acknowledgements

The authors like to express their thanks for the financial supports by National Nature Science Foundation of China (project No.31070871), National High Technology Research and Development Program (863) (project No.2008AA03Z305), Science and Technology Commission of Shanghai Municipality (project No. 11nm0506200) and the National Plan for Science and Technology (project No. 10-NAN1013-02).

## References

[1] Writing Group M., D. Lloyd-Jones, R.J. Adams, et al., Executive summary: heart disease and stroke statistics 2010 update: a report from the American Heart Association, Circulation 121 (7) (2010) 948–954.
[2] T.A. Mahmood, V.P. Shastri, C.A. Van Blitterswijk, et al., Tissue engineering of bovine articular cartilage within porous poly(ether ester) copolymer scaffolds with different structures, Tissue Engineering 11 (7–8) (2005) 1244–1253.
[3] M. Ehrenreich, Z. Ruszczak, Update on tissue-engineered biological dressings, Tissue Engineering 12 (9) (2006) 2407–2424.
[4] M.M. Stevens, J.H. George, Exploring and engineering the cell surface interface, Science 310 (5751) (2005) 1135–1138.
[5] Z.G. Chen, P.W. Wang, B. Wei, et al., Electrospun collagen–chitosan nanofiber: a biomimetic extracellular matrix for endothelial cell and smooth muscle cell, Acta Biomaterialia 6 (2) (2010) 372–382.

[6] R.Y. Kannan, H.J. Salacinski, P.E. Butler, et al., Current status of prosthetic bypass grafts: a review, Journal of Biomedical Materials Research Part B 74B (1) (2005) 570–581.
[7] B.C. Isenberg, C. Williams, R.T. Tranquillo, Small-diameter artificial arteries engineered in vitro, Circulation Research 98 (2006) 25–35.
[8] S.F. Badylak, The extracellular matrix as a biologic scaffold material, Biomaterials 28 (25) (2007) 3587–3593.
[9] C. Huang, R. Chen, Q. Ke, et al., Electrospun collagen–chitosan–PU nanofibrous scaffolds for tissue engineered tubular grafts, Colloids and Surfaces B 82 (2) (2011) 307–315.
[10] J. Hu, Z. Cai, Z. Zhou, Progress in studies on the characteristics of human amnion mesenchymal cells, Progress in Natural Science 19 (9) (2009) 1047–1052.
[11] Y. Cao, B. Zhang, T. Croll, et al., Engineering tissue tubes using novel multilayered scaffolds in the rat peritoneal cavity, Journal of Biomedical Materials Research Part A 87 (3) (2008) 719–727.
[12] A.P. Zhu, F. Zhao, N. Fang, Regulation of vascular smooth muscle cells on poly(ethylene terephthalate) film by O-carboxymethylchitosan surface immobilization, Journal of Biomedical Materials Research Part A 86A (2) (2008) 467–476.
[13] S.C. Bir, J. Esaki, A. Marui, et al., Angiogenic properties of sustained release platelet-rich plasma: characterization in-vitro and in the ischemic hind limb of the mouse, Journal of Vascular Surgery 50 (4) (2009) (870-9.e2).
[14] M. Hu, M. Kurisawa, R. Deng, et al., Cell immobilization in gelatin-hydroxyphenylpropionic acid hydrogel fibers, Biomaterials 30 (21) (2009) 3523–3531.
[15] Y. Wang, D.D. Rudym, A. Walsh, et al., In vivo degradation of three-dimensional silk fibroin scaffolds, Biomaterials 29 (24–25) (2008) 3415–3428.
[16] S. Weisman, H.E. Trueman, S.T. Mudie, et al., An unlikely silk: the composite material of green lacewing cocoons, Biomacromolecules 9 (11) (2008) 3065–3069.
[17] A. Doraiswamy, R.J. Narayan, Vascular tissue engineering by computer-aided laser micromachining, Philosophical Transactions of The Royal Society A 368 (1917) (2010) 1891–1912.
[18] C. Huang, Y. Tang, X. Liu, et al., Electrospinning of nanofibres with parallel line surface texture for improvement of nerve cell growth, Soft Matter 7 (2011) 10812–10817.
[19] C.P. Barnes, S.A. Sell, E.D. Boland, et al., Nanofiber technology: designing the next generation of tissue engineering scaffolds, Advanced Drug Delivery Reviews 59 (14) (2007) 1413–1433.
[20] K.S. Rho, L. Jeong, G. Lee, et al., Electrospinning of collagen nanofibers: effects on the behavior of normal human keratinocytes and early-stage wound healing, Biomaterials 27 (8) (2006) 1452–1461.
[21] R. Murugan, S. Ramakrishna, Nano-featured scaffolds for tissue engineering: a review of spinning methodologies, Tissue Engineering 12 (3) (2006) 435–447.
[22] B.W. Tillman, S.K. Yazdani, S.J. Lee, R.L. Geary, A. Atala, J.J. Yoo, The in vivo stability of electrospun polycaprolactone–collagen scaffolds in vascular reconstruction, Biomaterials 30 (4) (2009) 583–588.
[23] S.J. Lee, J.J. Yoo, G.J. Lim, A. Atala, J. Stitzel, In vitro evaluation of electrospun nanofiber scaffolds for vascular graft application, Journal of Biomedical Materials Research Part A 83A (4) (2007) 999–1008.
[24] J.D. Berglund, M.M. Mohseni, R.M. Nerem, A. Sambanis, A biological hybrid model for collagen-based tissue engineered vascular constructs, Biomaterials 249 (7) (2003) 1241–1254.
[25] S.A. Sell, M.J. McClure, C.P. Barnes, et al., Electrospun polydioxanone-elastin blends: potential for bioresorbable vascular grafts, Biomedical Materials 1 (2) (2006) 72–80.
[26] I.-S. Yeo, J.-E. Oh, L. Jeong, et al., Collagen-based biomimetic nanofibrous scaffolds: preparation and characterization of collagen/silk fibroin bicomponent nanofibrous structures, Biomacromolecules 9 (4) (2008) 1106–1116.
[27] X. Wang, L. Qiao, A. Horii, Screening of functionalized self-assembling peptide nanofiber scaffolds with angiogenic activity for endothelial cell growth, Progress in Natural Science: Materials International 21 (2) (2011) 111–116.
[28] D.L. Li, C.X. Pan, Fabrication and characterization of electrospun $TiO_2$/CuS micro-nano-scaled composite fibers, Progress in Natural Science: Materials International 22 (1) (2012) 59–63.